



Published in final edited form as:

*Vet Comp Oncol.* 2018 December ; 16(4): 606–615. doi:10.1111/vco.12428.

## Targeting NEDD8-activating enzyme is a new approach to treat canine diffuse large B-cell lymphoma

A. L. F. V. Assumpção<sup>1</sup>, Z. Lu<sup>1</sup>, K. W. Marlowe<sup>1</sup>, K. S. Shaffer<sup>1</sup>, and X. Pan<sup>1,2</sup>

<sup>1</sup>Department of Medical Sciences, School of Veterinary Medicine, University of Wisconsin-Madison, Madison, Wisconsin

<sup>2</sup>Carbone Cancer Center, University of Wisconsin-Madison, Madison, Wisconsin

### Abstract

Canine diffuse large B-cell lymphoma (DLBCL), the most common hematologic malignancy of dogs, is associated with poor overall survival. The lack of conventional chemotherapies with sustainable efficacy warrants investigation of novel therapies. Pevonedistat (MLN4924) is a potent and selective small molecule NEDD8-activating enzyme inhibitor. In human activated B-cell-like (ABC) diffuse large B-cell lymphoma, pevonedistat induces lymphoma cell apoptosis, DNA damage and G1 cell cycle arrest by inhibiting the nuclear factor- $\kappa$ B (NF- $\kappa$ B) pathway. Genomic and transcriptomic studies showed that the NF- $\kappa$ B pathway is deregulated in canine DLBCL. Our results showed that pevonedistat treatment significantly reduces the viability of canine DLBCL cells by inducing G1 cell cycle arrest and apoptosis. Pevonedistat treatment inhibits NF- $\kappa$ B pathway activation and downregulates NF- $\kappa$ B target genes in canine DLBCL. Moreover, administration of pevonedistat to mice bearing canine DLBCL xenograft tumours resulted in tumour regression. Our in vivo and in vitro studies provide justification for future clinical application of pevonedistat as a potential new anti-cancer therapy that may benefit both canine and human species.

### Keywords

canine; DLBCL; NAE-inhibitor; NF- $\kappa$ B pathway; xenograft tumour

## 1 | INTRODUCTION

Canine diffuse large B-cell lymphoma (DLBCL), the most common hematologic malignancy of dogs, is associated with poor overall survival due to the lack of conventional chemotherapies with sustainable efficacy.<sup>1</sup> While 90% of canine DLBCL patients initially respond to cyclophosphamide-doxorubicin-vincristine-prednisone (CHOP)-based

---

**Correspondence:** X. Pan, VMD, PhD, DACVIM (Oncology), School of Veterinary Medicine, University of Wisconsin-Madison, Department of Medical Sciences, 2015 Linden Dr., Madison, WI, 53706., xpan24@wisc.edu.

Conflict of interest

The authors declare no competing interests.

SUPPORTING INFORMATION

Additional supporting information may be found online in the Supporting Information section at the end of the article.

chemotherapy, the duration of response is short, with a median survival time of approximately 10 months.<sup>2,3</sup> The common occurrence and poor prognosis of canine DLBCL have mandated a great need for the investigation of new therapies. As canine DLBCL serves as a comparative model for human DLBCL,<sup>4,5</sup> development of new therapeutic treatments for DLBCL may benefit both species.

The development of targeted molecular therapies for canine DLBCL has resulted in renewed enthusiasm that extended survival time may be achievable, while limiting toxicities. Targeted therapy drugs interfere with the internal cell-signalling pathways unique to cancer cell proliferation or apoptosis, allowing the body's normal cells to be spared, and resulting in fewer side effects. The NEDD8-regulated ubiquitylation system plays essential functions in proteasomal degradation of intracellular proteins with important cellular functions. Three distinct enzymes mediate the NEDD8-regulated ubiquitylation pathway: NEDD8-activating enzyme (E1), NEDD8-conjugating enzyme (E2) and NEDD8-ligase enzyme (E3). NEDD8 is first activated by E1 enzyme, NEDD8 activating enzyme (NAE). The activated NEDD8 is then transferred from the E1 to E2. E2 then collaborates with E3, cullin-RING ligases (CRLs), to conjugate the NEDD8 to the substrate protein such as the inhibitor of NF- $\kappa$ B pathway, phosphorylated I $\kappa$ B $\alpha$  (p-I $\kappa$ B $\alpha$ ), or DNA replication enzyme Cdt-1 for degradation.<sup>6,7</sup> Pevonedistat (MLN4924) is a potent and selective small-molecule inhibitor of NEDD8-activating enzyme (NAE) that is currently in phase I clinical trials in people.<sup>8-11</sup> Pevonedistat potently inhibits NAE, resulting in inhibition of cullin-RING ligase (CRL neddylation) and a subsequent increase of CRL substrate proteins such as p-I $\kappa$ B $\alpha$ .<sup>12</sup> In most cancer cells, inhibition of NAE leads to an induction of DNA re-replication, S-phase cell cycle arrest, DNA damage and apoptosis.<sup>13</sup> However, in human activated B-cell-like (ABC) DLBCL, pevonedistat inhibits the NF- $\kappa$ B pathway and results in rapid accumulation of p-I $\kappa$ B $\alpha$ , reduction of NF- $\kappa$ B target gene expressions, G1 cell cycle arrest and cell apoptosis.<sup>14</sup> Administration of pevonedistat to mice bearing human xenograft ABC-DLBCL blocked the NF- $\kappa$ B pathway activation and led to complete regression of xenograft tumours.<sup>14</sup> Pevonedistat has shown a good safety profile in phase I clinical trials of people diagnosed with metastatic melanoma,<sup>11</sup> advanced solid tumour,<sup>9</sup> acute myeloid leukaemia, myelodysplastic syndromes,<sup>10</sup> lymphoma and multiple myeloma.<sup>8</sup> In phase I patients with relapsed/refractory lymphoma or multiple myeloma, clinically significant myelosuppression was rare and no treatment-related deaths occurred. With pevonedistat treatment, 33/34 patients achieved either partial responses or stable disease.<sup>8</sup> The promising clinical efficacy and generally manageable safety profile make pevonedistat an attractive agent for future clinical implications.

Clinical implementation of targeted therapies depends on a thorough understanding of which molecular or signalling pathways contribute to the survival, growth, metastasis and other malignant behaviours of specific tumour types. Our study aimed to evaluate *in vitro* and *in vivo* effects of pevonedistat treatment in canine DLBCL cells and canine DLBCL xenograft mice, and to elucidate the underlying mechanisms of pevonedistat-mediated anti-tumour effects.

## 2 | METHODS

### 2.1 | Primary canine DLBCL samples, cell lines and culture conditions

Lymph node samples were collected from client-owned dogs with a cytological diagnosis of multicentric large B-cell lymphoma or healthy dogs at Oncology Service of UW-Madison Teaching Hospital. Immunophenotype of DLBCL was confirmed by flow cytometry evaluation at Colorado State University. All canine lymphoma cells were aspirated using a 20 ga needle into C10 medium containing RPMI1640 with 10% FBS, 1 × Penicillin/Streptomycin, 1 × non-essential amino acids, 1 × L-glutamine, 1 mM sodium pyruvate, and 1 × HEPES. Cells were spun down at  $1.5 \times 10^3$  rpm (RPM) for 5 minutes at 4°C and were re-suspended in ACK lysis buffer for red blood cell lysis. Primary canine DLBCL or normal lymph node samples were cultured overnight in C10 medium, and only samples that survived and had healthy morphological appearance after initial overnight culture, were used for cell viability and apoptosis assays. All primary canine DLBCL cells were maintained in culture for less than 96 hours. The canine DLBCL cell line CLBL-1<sup>15</sup> was cultured in Iscove's Modified Dulbecco's Medium (IMDM) containing 20% fetal bovine serum (FBS), 1 × penicillin/streptomycin and 1 × L-glutamine. CLBL-1 cells were cultured at 37°C with 5% CO<sub>2</sub> and were passaged every 24 hours.

### 2.2 | Trypan blue exclusion assay

The CLBL-1 cells were seeded at a concentration of  $0.1 \times 10^6$  cells/mL in 6-well plates. Cells were treated with pevonedistat (Chemietek Indianapolis, IN) at doses of 0.25, 0.5 and 1 µM. Dimethyl sulfoxide (DMSO, 100%) was used as a negative control, and doxorubicin (0.3 µM) was used as a positive control. The viable cells were counted by trypan blue exclusion assay before the drug treatment, and after 24, 48 or 72-hour drug treatment. The percentage of viable cells was normalized to the DMSO-treated cell count.

### 2.3 | MTS assay and half maximal inhibitory concentration (IC<sub>50</sub>)

CLBL-1 and primary DLBCL cells were suspended to a final concentration of  $4 \times 10^5$  cells/mL or  $2 \times 10^6$  cells/mL, respectively in their culture medium. 100 µL (40 000 CLBL-1 or 200 000 primary cells) were dispensed per well of 96-well plates and quadruplicates were made for each treatment group. CLBL-1 cells or primary samples were treated with pevonedistat at concentrations of 0.25, 0.5, 1, 2 or 4 µM continuously for 48 or 72 hours, and 20 µL 3-(4,5-dimethylthiazol-2-yl)-5-(3-carboxymethoxyphenyl)-2-(4-sulfophenyl)-2H-tetrazolium/phenazine ethosulfate solution was added to each well after drug treatment. Plates were incubated at 37°C for 1 to 4 hours in a humidified, 5% CO<sub>2</sub> atmosphere. A 96-well plate reader recorded the absorbance at 490 nm. The optical density at 490 nm (OD<sub>490</sub>) of pevonedistat-treated groups was normalized by the OD<sub>490</sub> of DMSO control and results were plotted as the normalized OD<sub>490</sub> (Y-axis) vs the concentration of pevonedistat (X-axis). The IC<sub>50</sub> was defined as the concentration of pevonedistat necessary to give 50% of the inhibitory response, and the IC<sub>90</sub> was defined as the concentration of pevonedistat necessary to give 90% of the inhibitory response. IC<sub>50</sub> and IC<sub>90</sub> were calculated using GraphPad Prism v6.05.

## 2.4 | Apoptosis assay

After 72-hours of drug treatment, CLBL-1 cells treated with DMSO or pevonedistat at concentrations of 0.25, 0.5 and 1.0  $\mu\text{M}$  were collected and were stained with FITC-conjugated Annexin V (1:40; eBioscience, Inc., San Diego, CA) and SYTOX DNA binding dye (1:1000; Thermo Fisher Scientific, Madison, WI). Primary DLBCL samples treated with DMSO or pevonedistat (2.0  $\mu\text{M}$ ) were harvested after 12 hours of treatment and stained with fluorescein isothiocyanate (FITC)-conjugated Annexin V (1:40; eBioscience, Inc., San Diego, CA) and DAPI (1:500; Thermo Fisher Scientific, Madison, WI) and were subjected to evaluation by flow cytometry. Samples were analysed using BD LSRII flow cytometry machine (BD Biosciences, San Jose, CA), and results were analysed using FlowJo v10.0.7 software.

## 2.5 | Cell proliferation assay

$0.5 \times 10^6$  CLBL-1 cells were harvested after 72-hour of DMSO or pevonedistat treatment. Cells first were stained with the fixable viability dye, Ghost Dye Red 780 (1:1000; Tonbo Biosciences, San Diego, CA). For intracellular Ki67 staining, cells were fixed and permeabilized using the BD Cytotfix/Cytoperm kit (BD Biosciences, San Jose, CA) and further labelled with FITC anti-Ki67 (1:20; BD Biosciences, San Jose, CA). DAPI solution (1:250; Thermo Fisher Scientific, Madison, WI) was then added and incubated overnight at 4°C. Samples were analysed on a BD LSRFortessa (BD Biosciences, San Jose, CA), and results were analysed using FlowJo v10.0.7 software.

## 2.6 | Western blot

The CLBL-1 cells were treated with DMSO control or pevonedistat (0.1–0.7  $\mu\text{M}$ ) for 1, 4, 6, 12 or 24 hours. Cell lysates were made according to the previously published methods<sup>16</sup> and were described in detail in the supplementary data. For detection of p-I $\kappa$ B $\alpha$ , CLBL-1 cells were stimulated with 10 ng/mL of human recombinant (rh) TNF $\alpha$  (PeproTech, Rocky Hill, NJ) for 5 minutes before preparing cell lysates in both pevonedistat and DMSO-treated groups. For detection of cleaved Caspase 3, and phosphorylated Histone 2AX, cells were not stimulated with any cytokine. The following commercial antibodies were used in western blots: p-I $\kappa$ B $\alpha$  (1:1000, Cell Signalling Technology, Danvers, MA, 14D4), cleaved caspase-3 (1:1000, Cell Signalling Technology, Danvers, MA, 5A1E) and p-H2AX (1:1000, Santa Cruz Biotechnology, Dallas, TX, sc-517348), and  $\beta$ -actin (1:5000, Sigma-Aldrich, AC-15).

## 2.7 | Generation of canine DLBCL xenograft mice

NOD-Prkdc<sup>SCID</sup> IL2rg<sup>null</sup> (NSG) mice were obtained from the Jackson Laboratories. All experiments involving animals were approved by the IACUC of the University of Wisconsin-Madison and conform to the appropriate regulatory standards. 10-week-old NSG mice were injected with  $2 \times 10^6$  CLBL-1 cells subcutaneously at the flank region, and tumour growth was monitored daily with calliper measurement. Once the mean tumours reached approximately 300 mm<sup>3</sup>, mice were treated with subcutaneous injections of 10%  $\beta$ -cyclodextrin or pevonedistat (60 mg/kg) at the opposite side of the flank to avoid intratumour injection.

## 2.8 | Reverse transcription and quantitative real-time PCR (qRT-PCR)

CLBL-1 or primary DLBCL cells were treated with DMSO or pevonedistat (0.58  $\mu\text{M}$  or 2  $\mu\text{M}$ ) for 1, 3, 12 or 24 hours. Total RNA was isolated with PureLink RNA Mini kit (Life Technologies Corporation, Carlsbad, CA) according to the standard manufacturer's protocol. Complementary DNA (cDNA) was synthesized with SuperScript III First-Strand System Kit (Life Technologies Corporation, Carlsbad, CA) with oligo (dT) primers. *TNF*, *Bcl-2*, *c-Flip*, *I $\kappa$ B $\alpha$* , *XIAP* and *A1* transcripts were detected by Roche Lightcycler96 with the cycle setting at 95°C (10 minutes), 95°C (10 seconds), 60°C (10 seconds) and 72°C (20 seconds) for a total of 40 cycles. *Gapdh* was used as an internal control for normalization, and quantification was determined by the delta-delta cycle threshold ( $\Delta\Delta\text{Ct}$ ) method. The primer sequences were previously described and listed in Appendix S1 (Supporting information).<sup>16,17</sup>

## 2.9 | Statistical analysis

All statistical analyses were conducted using GraphPad Prism v6.05<sup>c</sup>. Two-way analysis of variance (ANOVA) followed by Dunnett's multiple comparisons was used in Trypan blue and MTS assays. Two-way ANOVA followed by Tukey's post hoc test was used in apoptosis and proliferation assays in CLBL-1 cells. Unpaired *t*-test was used in primary DLBCL cell apoptosis assay, and in xenograft tumour weight evaluation. For xenograft tumour volume evaluation, a mixed model equation was performed with the following assumptions:  $y = \beta_1\text{Treatment} + \beta_2\text{Day} + \beta_3 : i, a + e$ . With fixed effects for treatment level and day of measurement, and animal measure as a random effect in nesting in the interaction between treatment and day. *P* values  $\leq 0.05$  were considered statistically significant. The heat map plots were generated by R version 3.4.3 statistical software with the packages ggplot2 via the function *geom\_raster*.

## 3 | RESULTS

### 3.1 | Pevonedistat inhibits canine DLBCL cell growth in vitro

To assess whether pevonedistat inhibits canine DLBCL cell growth in vitro, canine DLBCL cell line CLBL-1<sup>15</sup> was treated with pevonedistat or DMSO control. Trypan blue exclusion assay showed that CLBL-1 cells treated with pevonedistat had a significant reduction of viable cells compared with the DMSO control. Pevonedistat-mediated inhibition of canine DLBCL cell growth was dose- and time-dependent as there was a gradual decrease of viable cells with increasing drug concentration and treatment time (Figure 1A). At higher concentrations (0.5 and 1.0  $\mu\text{M}$ ) and longer incubation time (Day 2 and 3), pevonedistat treatment had a similar efficacy of inhibiting DLBCL cell growth as cytotoxic chemotherapy drug doxorubicin (Figure 1A). Consistent with the trypan blue exclusion assay, CellTiter96 AQueous One Solution Cell Proliferation assay showed a significant dose- and time-dependent reduction of CLBL-1 cell growth after 48 or 72 hours of drug treatment compared with the DMSO control (Figure 1B). To further quantify the concentration of pevonedistat necessary to give 50% (IC<sub>50</sub>) and 90% (IC<sub>90</sub>) of the inhibitory response, CLBL-1 cells were treated with pevonedistat at concentrations of 0–1.2  $\mu\text{M}$  for 72 hours. MTS assay was conducted and the OD<sub>490</sub> of pevonedistat-treated groups were normalized by the OD<sub>490</sub> of the DMSO control. The IC<sub>50</sub> and IC<sub>90</sub> of pevonedistat with 72-hours treatment were 0.323

$\mu\text{M}$  and  $0.582 \mu\text{M}$ , respectively (Figure 1C). Our results showed that pevonedistat efficiently inhibits CLBL-1 cell growth in a dose-and time-dependent manner.

### 3.2 | Pevonedistat decreases the viability of primary canine DLBCL patient samples

As CLBL-1 is the only well- established and characterized canine DLBCL cell line,<sup>15</sup> primary canine DLBCL samples were utilized to assess the impact of pevonedistat treatment on cell viability. Lymphoma cells or normal lymphocytes were aspirated from peripheral lymph nodes of four dogs diagnosed with multicentric large B-cell lymphoma and three healthy dogs at the Oncology Service of UW-Madison Veterinary Care. Lymphoma diagnosis and immunophenotype were confirmed by cytological evaluation, immunocytochemistry and flow cytometry by board-certified veterinary pathologists. Compared with the DMSO control group, all primary canine DLBCL samples had a significant reduction of viable cells when treated with 1 and 2  $\mu\text{M}$  pevonedistat for 72 hours. Three out of four patient samples had a significant decrease of cell viability when treated with 0.5  $\mu\text{M}$  pevonedistat (Patients 1, 2 and 4) for 72 hours (Figure 2A). With as short as 24-hours treatment, we observed a reduction of cell number/density in pevonedistat-treated samples (Figure S1). In contrast, pevonedistat treatment did not impact cell viability of normal lymphocytes even with 72 hours treatment and at a high concentration of 4  $\mu\text{M}$  (Figure 2B). Our data support that pevonedistat treatment decreases the cell viability of primary canine DLBCL samples and spares normal lymphocytes.

### 3.3 | Pevonedistat promotes cell apoptosis in canine DLBCL

To explore underlying mechanisms by which pevonedistat decreased canine DLBCL cell viability, we performed apoptosis assay to determine if reduction of DLBCL cell number occurred as a consequence of increased apoptosis. CLBL-1 cells were treated with DMSO or pevonedistat (0.25, 0.5, and 1  $\mu\text{M}$ ) for 72 hours, stained with Annexin V and SYTOX Red dead cell stain, and subjected to flow cytometry analysis. Early apoptotic cells were defined as Annexin V-positive and SYTOX Red dead cell stain-negative. Healthy cells were defined as double negative for both Annexin V and SYTOX Red dead cell stains. Late apoptotic cells were defined as double positive for both Annexin V and SYTOX Red dead cell stain (Figure 3A). While percentages of healthy cells were decreased in pevonedistat-treated groups, percentages of early apoptotic cell were increased compared to the DMSO control (Figures 3A,B). Moreover, pro-apoptotic protein cleaved caspase-3 increased with higher concentration and longer treatment time of pevonedistat (Figure 3C). Next, we tested whether pevonedistat treatment impacts apoptosis in primary canine DLBCL samples. After 12 hours pevonedistat treatment at 2  $\mu\text{M}$ , all four primary canine DLBCL samples had a significant increase of early apoptotic cells (Figure 3D). Thus, pevonedistat treatment increases apoptosis in canine DLBCL cell and primary DLBCL samples.

### 3.4 | Pevonedistat disrupts canine DLBCL cell proliferation cycle and leads to DNA damage

Inhibition of cell growth can be achieved by increasing cell apoptosis, by decreasing cell proliferation, or by both mechanisms. We further assessed the impact of pevonedistat treatment on the cell cycle of canine DLBCL cells. CLBL-1 cells were treated with DMSO or pevonedistat (0.25, 0.5, and 1  $\mu\text{M}$ ) for 72 hours. Cells in quiescent phase (G0) were



defined as Ki67-negative and DAPI-negative. Cells in G1 phase were defined as Ki67-positive and DAPI-negative. Cells in S/G2/M were defined as Ki67-positive and DAPI-positive (Figure 4A). Pevonedistat-treated canine CLBL-1 cells had an increased percentage of cells in G1 and a decreased percentage of cells in S/G2/M phases compared with the DMSO control, and higher concentration of pevonedistat treatment led to more cells that were arrested at the G1 phase (Figure 4B). Additionally, evidence of DNA damage was detected in pevonedistat-treated CLBL-1 cells as shown by phosphorylation of ATM substrate p-H2AX (Figure 4C). Pevonedistat-mediated DNA damage was time- and dose-dependent as p-H2AX increased with higher concentration of drug and longer treatment time. Thus, pevonedistat causes G1-cell-cycle arrest and DNA damage in canine DLBCL cells.

### 3.5 | Pevonedistat inhibits NF- $\kappa$ B pathway in canine DLBCL cells

The nuclear factor- $\kappa$ B (NF- $\kappa$ B) pathway plays a key role in tumorigenesis and progression through transcriptional control of genes involved in cell growth, apoptosis, angiogenesis, metastasis and cell migration.<sup>18</sup> In the canonical NF- $\kappa$ B pathway, NF- $\kappa$ B transcription factors are sequestered in an inactive state in cytoplasm by binding to the inhibitor of NF- $\kappa$ B $\alpha$  (I $\kappa$ B $\alpha$ ). Upon stimulation of the IKK complex, I $\kappa$ B $\alpha$  is phosphorylated, resulting in its polyubiquitination and degradation, thus subsequent activation of the NF- $\kappa$ B pathway.<sup>19,20</sup> Regulation of NF- $\kappa$ B signalling occurs at many levels, one of which is through the regulation of turnover of p-I $\kappa$ B $\alpha$  by NEDD8-regulated ubiquitinylation and proteasomal degradation.<sup>21</sup> The cytoplasmic accumulation of p-I $\kappa$ B $\alpha$  prevents nuclear translocation of NF- $\kappa$ B transcription factors and inactivates the NF- $\kappa$ B pathway. In pevonedistat-treated CLBL-1 cells, p-I $\kappa$ B $\alpha$  protein expression was increased in a dose- and time-dependent manner (Figure 5A). Moreover, NF- $\kappa$ B pathway target genes, TNF, Bcl-2, c-Flip, XIAP and A1<sup>14,17,22</sup> were down-regulated after 24 hours pevonedistat treatment. I $\kappa$ B $\alpha$  was down regulated at 12 hours post-treatment and then increased at 24 hours post-treatment (Figure 5B). In primary canine DLBCL samples, Bcl-2, c-Flip and A1 were down-regulated in all five patient samples after 24 hours pevonedistat treatment. TNF was down-regulated in four out of five patient samples. I $\kappa$ B $\alpha$  and XIAP were down-regulated in two of five samples (Figure 5C). Therefore, pevonedistat inhibits the turn-over of p-I $\kappa$ B $\alpha$ , down regulates NF- $\kappa$ B target genes and inactivates NF- $\kappa$ B pathway in canine DLBCL cells and primary samples.

### 3.6 | Pevonedistat inhibits canine DLBCL xenograft tumour growth and leads to tumour regression

To examine the anti-tumor activity of pevonedistat in vivo, we generated a canine DLBCL xenograft mouse model by injecting CLBL-1 cells subcutaneously to NOD-Prkdc<sup>SCID</sup> IL2rg<sup>null</sup> (NSG) mice. The NSG mice are severely immunodeficient, completely lacking both adaptive and innate immune systems, which makes them highly receptive to engraftment of tumour cells.<sup>23</sup> After tumour formation at the injection sites, at around 14 to 16 days post-tumour cell injection, xenograft tumours were harvested to evaluate the morphology, immunophenotype and cell surface expression markers. Xenograft tumours had typical large B-cell lymphoma cytologic and histologic morphologies (Figure 6A), and tumour cells were monoclonal for immunoglobulin heavy major chain (Figure 6B). Flow

cytometry analysis revealed that xenograft tumour cells have a similar cell surface expressing markers as CLBL-1 cells and they were CD79<sup>+</sup> and CD3<sup>-</sup> (Figure 6C). We concluded that xenograft tumours recapitulate canine DLBCL cell morphology, immunophenotype and cell surface expression markers. Once xenograft tumours were established (reached ~300 mm<sup>3</sup>), subcutaneous administration of pevonedistat was started twice daily at dose of 60 mg/kg. Compared with mice injected with the vehicle control, mice treated with pevonedistat were able to reach a complete tumour regression after 10-days of treatment (Figure 6D,F). The tumour volume of the pevonedistat-treated mice was significantly decreased compared to the vehicle-treated group ( $P = 1.38e^{-06}$ ). At 28 days after starting drug treatment, there was a significant decrease of tumour weight in pevonedistat-treated mice ( $P = 0.0322$ ) (Figure 6E). Among three mice received pevonedistat treatment, xenograft tumour regrew in one mouse at day 15 after treatment. Post-mortem exam revealed that most mice (4/5) received vehicle treatment developed intrabdominal and axillary lymphadenopathy. In contrast, no abdominal lymphadenopathy was detected in mice treated with pevonedistat. The mouse that regrew subcutaneous xenograft tumour had axillary lymphadenopathy upon necropsy (Figure S2A, B). There was no statistical difference in spleen and liver weights comparing pevonedistat vs vehicle-treated mice (Figure S2C, D). Interestingly, four out of six NF- $\kappa$ B pathway target genes (TNF, Bcl-2, c-Flip and A1) were significantly down-regulated in xenograft tumours 48 hours after mice treated with one dose of pevonedistat treatment (60 mg/kg) (Figure 6G). Thus, pevonedistat inhibits canine DLBCL growth and downregulates NF- $\kappa$ B target genes in vivo.

## 4 | DISCUSSION

Pevonedistat is a novel first-class NAE inhibitor that has potent activity in malignant melanoma,<sup>11</sup> advanced solid tumour,<sup>9</sup> acute myeloid leukaemia, myelodysplastic syndromes,<sup>10</sup> lymphoma and multiple myeloma<sup>8</sup> in people. As canine DLBCL is an excellent large animal model for human DLBCL, our study assessed pevonedistat treatment impact on canine DLBCL cell proliferation and survival. Our data supports that pevonedistat has a broad tumoricidal activity against the canine DLBCL cell line (Figure 1) and primary canine DLBCL samples (Figure 2). The IC<sub>50</sub> of pevonedistat in canine DLBCL cells are within the nanomolar range (Figures 1C). *in vivo* xenograft model of canine DLBCL showed that pevonedistat treatment inhibits tumour growth and results in complete xenograft tumour regression after 10 days of drug treatment (Figure 6F). Nanomolar IC<sub>50</sub> and great *in vitro* anti-tumor efficacy support the conclusion that pevonedistat is a potent small molecule inhibitor for canine DLBCL.

Recent large-scale genome-wide studies show that NF- $\kappa$ B pathway is deregulated in canine DLBCL.<sup>23-26</sup> In a study of whole exome sequencing of B-cell lymphoma in Golden Retrievers, many mutated genes identified are involved in the canonical NF- $\kappa$ B pathway.<sup>23</sup> Recurrent gene mutations have also been described in NF- $\kappa$ B related pathway in 50% of the cocker spaniel B-cell lymphomas and 30% of all golden retriever B-cell lymphoma.<sup>26</sup> Gene expression profiles comparing canine DLBCL to normal lymph nodes reveal that NF- $\kappa$ B target genes are up-regulated in canine DLBCL.<sup>24</sup> Tissue arrays and immunohistochemistry further confirm that the NF- $\kappa$ B pathway is constitutively activated in canine DLBCL.<sup>27</sup>



Proteasome inhibitor Bortezomib suppresses NF- $\kappa$ B pathway activation and inhibits cell proliferation of canine DLBCL cell lines.<sup>28</sup> A synthetic NF- $\kappa$ B inhibitor IMD-0354 improves glucocorticoid sensitivity of canine malignant lymphoid cells by upregulating expression of glucocorticoid receptors.<sup>29</sup> Constitutively activated NF- $\kappa$ B signalling can also be inhibited by NEMO Binding Domain (NBD) peptide, which blocks NF- $\kappa$ B signalling.<sup>30</sup> NBD peptide administration to dogs with relapsed B-cell lymphoma can inhibit the expression of NF- $\kappa$ B target genes and reduce tumour burden.<sup>22</sup> These data support further investigation of NF- $\kappa$ B-targeted therapeutics in canine DLBCL. Our study here supports that pevonedistat induced cell apoptosis and cell cycle arrest by inhibiting NF- $\kappa$ B pathway. Thus, combination therapy of pevonedistat and NBD peptide may add synergistic effect for treating canine DLBCL. Despite the low IC<sub>50</sub> value in the canine lymphoma cell line, primary canine DLBCL samples had viable sensitivities to pevonedistat treatment (Figure 2). Due to heterogeneity in canine DLBCL, the treatment response to cytotoxic chemotherapy treatment always varies.<sup>31</sup> The sensitivity variations between patient samples suggest that individual DLBCL patients may respond to pevonedistat treatment differently. The status of NF- $\kappa$ B signalling in patient samples may impact the sensitivity of pevonedistat treatment. Canine DLBCL with high constitutive NF- $\kappa$ B signalling may have better responses to pevonedistat treatment than those with low or normal signalling. Due to the complexity and cross-talk between different signalling pathways, targeted therapies may result in the unintended activation of non-targeted signalling pathways, which in turn contribute to therapeutic resistance. The molecular determinants for pevonedistat drug sensitivity may be beyond the scope of canonical NF- $\kappa$ B signalling. Recent study showed that the alternative NF- $\kappa$ B pathway (ANF- $\kappa$ BP) is constitutively active in primary canine DLBCL samples, contributes to lymphoma cell survival and may serve as a therapeutic target.<sup>32</sup> Thus, ANF- $\kappa$ BP signalling status may also impact patient response to pevonedistat treatment. Comparing gene expression profiles from patient samples with differing drug sensitivities can identify biomarkers which may serve as a predictive screening tool to direct personalized anti-cancer treatment. There may be a distinct gene expression profile in pevonedistat-sensitive DLBCL and molecular profiling of canine lymphoma samples may allow for tailoring medical care to that individual need and provide a personalized therapy by stratifying disease status.

The primary mechanism of action of NAE inhibition in many cell types is through induction of DNA re-replication by blocking degradation of Cdt-1, a critical factor required for licensing origins of DNA replication. In most cancer cells, inhibition of NAE leads to induction of DNA re-replication, and then subsequent DNA damage and cell death.<sup>12,13</sup> In germinal center B-cell-like (GCB) DLBCL in people, pevonedistat treatment results in accumulation of cells in S-phase, consistent with cells undergoing DNA re-replication. However, in ABC-DLBCL, pevonedistat treatment results in a distinct G1-phase cell cycle arrest and apoptosis induction by inhibiting the canonical NF- $\kappa$ B pathway.<sup>14</sup> Because pevonedistat treatment causes G1-phase arrest, accumulation of p-I $\kappa$ B $\alpha$  and downregulation of NF- $\kappa$ B target genes (Figures 4 and 5), inhibition of the NF- $\kappa$ B pathway plays a critical role in pevonedistat-mediated anti-tumour effects in our study. As canine DLBCL is a heterogeneous disease with many different sub-types, deregulation of NF- $\kappa$ B pathway may not be the key driver for every subtype of canine DLBCL. Pevonedistat may inhibit canine

DLBCL primary samples by both NF- $\kappa$ B inhibition and induction of DNA damage depending on the specific tumour subtype. Future further characterization and classification of the primary canine DLBCL samples will lead to more in-depth studies of the underlying mechanisms governing the pevonedistat-mediated anti-tumour effects.

In our study, we generated a canine DLBCL murine xenograft model and utilized it to test the therapeutic effects of pevonedistat. Our xenograft model recapitulates canine large B-cell lymphoma in terms of the gross morphology, cytologic and histologic appearance, immunophenotype and cell surface expression markers. Within a 2-week period, the xenograft tumours reached  $\sim 300 \text{ mm}^3$  at all injection sites and mice bearing the xenograft tumour were able to maintain acceptable quality of life without treatment. Consistent with previous canine DLBCL xenograft models,<sup>33,34</sup> evaluation of the size of xenograft tumours provides an easy way to monitor the tumour growth, regression and regrowth throughout the treatment period. Thus, our study provides a great mouse model for future drug screening or mechanism studies. Although post-mortem study revealed that intrabdominal and axillary lymph nodes responded to pevonedistat treatment as well as xenograft tumours, the lack of thorough histopathology evaluation of spleen, liver, abdominal lymph nodes limited our ability to conclude that mice received pevonedistat were completely disease-free after 10 days treatment. Other limitation includes the relative small number of mice were treated with pevonedistat. We had total six mice treated with pevonedistat with three treated for 20 days (Figures 6D–F) and three treated with one dose (Figure 6G). In our *in vivo* study, one pevonedistat treated mouse exhibited tumour regrowth at 15 days after the treatment started. Future studies with increased numbers of treated mice and with longer follow-up time will help to further elucidate the molecular signatures and mechanisms of pevonedistat-associated therapeutic effect and drug resistance. Furthermore, future studies will forge new avenues for understanding the cross-talk between different signalling pathways in both canine and human DLBCL—avenues which almost certainly will provide a foundation for developing novel strategies and advancing fundamental knowledge.

#### 4.1 | Conclusion

Our study determined that an NAE inhibitor, pevonedistat effectively inhibits canine diffuse large B-cell lymphoma cell growth by promoting cell apoptosis and introducing a G1-phase cell cycle arrest. Pevonedistat inhibits the NF- $\kappa$ B pathway activation and downregulates the NF- $\kappa$ B target genes. *in vivo* administration of pevonedistat to canine DLBCL xenograft mice results in xenograft tumour regression. Our study will provide justification for further safety and efficacy studies of pevonedistat in DLBCL of dogs.

### Supplementary Material

Refer to Web version on PubMed Central for supplementary material.

### ACKNOWLEDGEMENTS

We thank Dr. Barbara Rutgen and Dr. Jaime Modiano for providing the canine CLBL-1 cell line. The work was conducted at the University of Wisconsin-Madison, and was supported by startup funds from UW-Madison, NIH K01OD020153–01A1 and UW-Madison Companion Animal Fund and Science without Borders (Capes—Brazil).

We would like to thank the University of Wisconsin Carbone Comprehensive Cancer Center (UWCCC) for use of its Shared Services (Flow Core Lab) to complete this research.

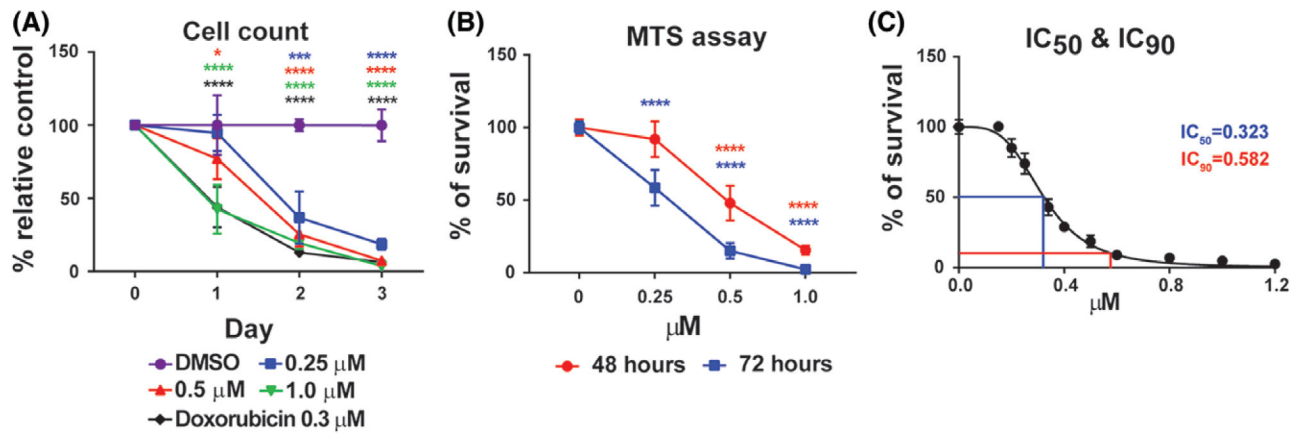
#### Funding information

Coordenação de Aperfeiçoamento de Pessoal de Nível Superior; NIH Office of the Director, Grant/Award Number: K01OD020153-01A1; University of Wisconsin-Madison, Grant/Award Number: Companion Animal Fund

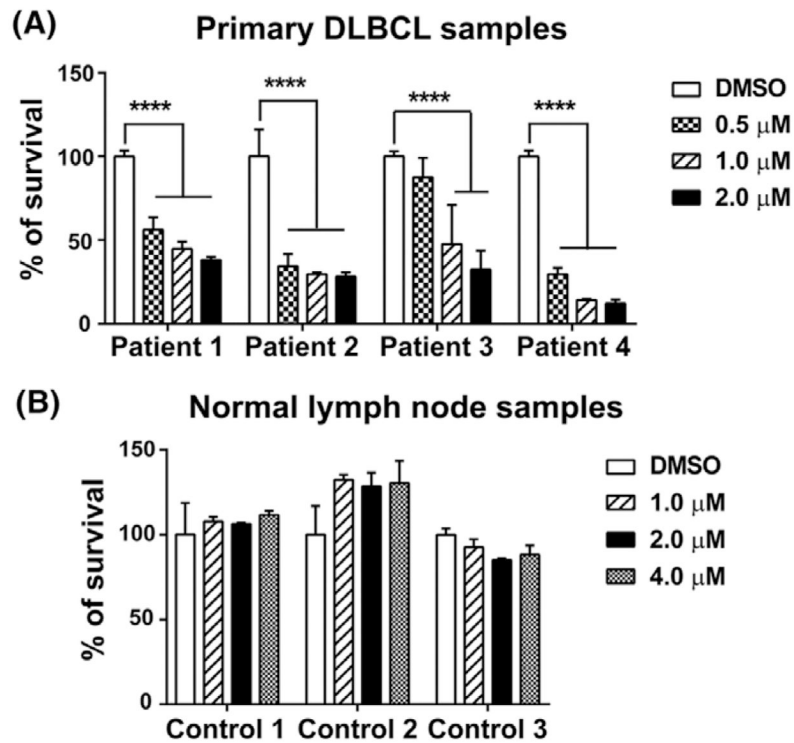
## REFERENCES

- Valli VE, San Myint M, Barthel A, et al. Classification of canine malignant lymphomas according to the World Health Organization criteria. *Vet Pathol.* 2011;48(1):198–211. [PubMed: 20861499]
- Valerius KD, Ogilvie GK, Mallinckrodt CH, Getzy DM. Doxorubicin alone or in combination with asparaginase, followed by cyclophosphamide, vincristine, and prednisone for treatment of multicentric lymphoma in dogs: 121 cases (1987–1995). *J Am Vet Med Assoc.* 1997; 210(4):512–516. [PubMed: 9040837]
- Keller ET, MacEwen EG, Rosenthal RC, Helfand SC, Fox LE. Evaluation of prognostic factors and sequential combination chemotherapy with doxorubicin for canine lymphoma. *J Veterinary Inter Med.* 1993;7(5): 289–295.
- Breen M, Modiano JF. Evolutionarily conserved cytogenetic changes in hematological malignancies of dogs and humans--man and his best friend share more than companionship. *Chromosom Res.* 2008;16(1): 145–154.
- Thomas R, Seiser EL, Motsinger-Reif A, et al. Refining tumor-associated aneuploidy through ‘genomic recoding’ of recurrent DNA copy number aberrations in 150 canine non-Hodgkin lymphomas. *Leuk Lymphoma.* 2011;52(7):1321–1335. [PubMed: 21375435]
- Pan ZQ, Kentsis A, Dias DC, Yamoah K, Wu K. NedD8 on cullin: building an expressway to protein destruction. *Oncogene.* 2004;23(11): 1985–1997. [PubMed: 15021886]
- Petroski MD, Deshaies RJ. Function and regulation of cullin-RING ubiquitin ligases. *Nat Rev Mol Cell Biol.* 2005;6(1):9–20. [PubMed: 15688063]
- Shah JJ, Jakubowiak AJ, O’Connor OA, et al. Phase I study of the novel investigational NEDD8-activating enzyme inhibitor pevonedistat (MLN4924) in patients with relapsed/refractory multiple myeloma or lymphoma. *Clin Cancer Res.* 2016;22(1):34–43. [PubMed: 26561559]
- Sarantopoulos J, Shapiro GI, Cohen RB, et al. Phase I study of the investigational NEDD8-activating enzyme inhibitor Pevonedistat (TAK-924/MLN4924) in patients with advanced solid tumors. *Clin Cancer Res.* 2016;22(4):847–857. [PubMed: 26423795]
- Swords RT, Erba HP, DeAngelo DJ, et al. Pevonedistat (MLN4924), a first-in-class NEDD8-activating enzyme inhibitor, in patients with acute myeloid leukaemia and myelodysplastic syndromes: a phase 1 study. *Br J Haematol.* 2015;169(4):534–543. [PubMed: 25733005]
- Bhatia S, Pavlick AC, Boasberg P, et al. A phase I study of the investigational NEDD8-activating enzyme inhibitor pevonedistat (TAK-924/MLN4924) in patients with metastatic melanoma. *Investig New Drugs.* 2016;34(4):439–449. [PubMed: 27056178]
- Soucy TA, Smith PG, Milhollen MA, et al. An inhibitor of NEDD8-activating enzyme as a new approach to treat cancer. *Nature.* 2009;458(7239):732–736. [PubMed: 19360080]
- Lin JJ, Milhollen MA, Smith PG, Narayanan U, Dutta A. NEDD8-targeting drug MLN4924 elicits DNA rereplication by stabilizing Cdt1 in S phase, triggering checkpoint activation, apoptosis, and senescence in cancer cells. *Cancer Res.* 2010;70(24):10310–10320. [PubMed: 21159650]
- Milhollen MA, Traore T, Adams-Duffy J, et al. MLN4924, a NEDD8-activating enzyme inhibitor, is active in diffuse large B-cell lymphoma models: rationale for treatment of NF- $\kappa$ B-dependent lymphoma. *Blood.* 2010;116(9):1515–1523. [PubMed: 20525923]
- Rutgen BC, Hammer SE, Gerner W, et al. Establishment and characterization of a novel canine B-cell line derived from a spontaneously occurring diffuse large cell lymphoma. *Leuk Res.* 2010;34(7):932–938. [PubMed: 20153049]
- Lu Z, Hong CC, Jark PC, et al. JAK1/2 inhibitors AZD1480 and CYT387 inhibit canine B-cell lymphoma growth by increasing apoptosis and disrupting cell proliferation. *J Vet Intern Med.* 2017;31: 1804–1815. [PubMed: 28960447]

17. Gaurnier-Hausser A, Patel R, Baldwin AS, May MJ, Mason NJ. NEMO-binding domain peptide inhibits constitutive NF-kappaB activity and reduces tumor burden in a canine model of relapsed, refractory diffuse large B-cell lymphoma. *Clin Cancer Res.* 2011;17(14): 4661–4671. [PubMed: 21610150]
18. Karin M, Cao Y, Greten FR, Li ZW. NF-kappaB in cancer: from innocent bystander to major culprit. *Nat Rev Cancer.* 2002;2(4):301–310. [PubMed: 12001991]
19. Campbell KJ, Rocha S, Perkins ND. Active repression of antiapoptotic gene expression by RelA(p65) NF-kappa B. *Mol Cell.* 2004;13(6): 853–865. [PubMed: 15053878]
20. Mercurio F, Zhu H, Murray BW, et al. IKK-1 and IKK-2: cytokine-activated IkappaB kinases essential for NF-kappaB activation. *Science.* 1997;278(5339):860–866. [PubMed: 9346484]
21. Read MA, Brownell JE, Gladysheva TB, et al. Nedd8 modification of cul-1 activates SCF(beta[TrCP])-dependent ubiquitination of Ikappa-Balpha. *Mol Cell Biol.* 2000;20(7):2326–2333. [PubMed: 10713156]
22. Habineza Ndikuyeze G, Gaurnier-Hausser A, Patel R, et al. A phase I clinical trial of systemically delivered NEMO binding domain peptide in dogs with spontaneous activated B-cell like diffuse large B-cell lymphoma. *PLoS One.* 2014;9(5):e95404. [PubMed: 24798348]
23. Tonomura N, Elvers I, Thomas R, et al. Genome-wide association study identifies shared risk loci common to two malignancies in golden retrievers. *PLoS Genet.* 2015;11(2):e1004922. [PubMed: 25642983]
24. Mudaliar MA, Haggart RD, Miele G, et al. Comparative gene expression profiling identifies common molecular signatures of NF-kappaB activation in canine and human diffuse large B cell lymphoma (DLBCL). *PLoS One.* 2013;8(9):e72591. [PubMed: 24023754]
25. Bushell KR, Kim Y, Chan FC, et al. Genetic inactivation of TRAF3 in canine and human B-cell lymphoma. *Blood.* 2015;125(6):999–1005. [PubMed: 25468570]
26. Elvers I, Turner-Maier J, Swofford R, et al. Exome sequencing of lymphomas from three dog breeds reveals somatic mutation patterns reflecting genetic background. *Genome Res.* 2015;25(11):1634–1645. [PubMed: 26377837]
27. Richards KL, Motsinger-Reif AA, Chen HW, et al. Gene profiling of canine B-cell lymphoma reveals germinal center and postgerminal center subtypes with different survival times, modeling human DLBCL. *Cancer Res.* 2013;73(16):5029–5039. [PubMed: 23783577]
28. Kojima K, Fujino Y, Goto-Koshino Y, Ohno K, Tsujimoto H. Analyses on activation of NF-kappaB and effect of bortezomib in canine neo-plastic lymphoid cell lines. *J Vet Med Sci.* 2013;75(6):727–731. [PubMed: 23337362]
29. Matsuda A, Tanaka A, Muto S, et al. A novel NF-kappaB inhibitor improves glucocorticoid sensitivity of canine neoplastic lymphoid cells by up-regulating expression of glucocorticoid receptors. *Res Vet Sci.* 2010;89(3):378–382. [PubMed: 20362310]
30. Gaurnier-Hausser A, Mason NJ. Assessment of canonical NF-kappaB activity in canine diffuse large B-cell lymphoma. *Methods Mol Biol.* 2015;1280:469–504. [PubMed: 25736768]
31. Paoloni M, Webb C, Mazcko C, et al. Prospective molecular profiling of canine cancers provides a clinically relevant comparative model for evaluating personalized medicine (PMed) trials. *PLoS One.* 2014;9(3): e90028. [PubMed: 24637659]
32. Seelig DM, Ito D, Forster CL. Constitutive activation of alternative nuclear factor kappa B pathway in canine diffuse large B-cell lymphoma contributes to tumor cell survival and is a target of new adjuvant therapies. *Leuk Lymphoma.* 2017;58(7):et al., 1702–1710. [PubMed: 27931134]
33. Rutgen BC, Willenbrock S, Reimann-Berg N, et al. Authentication of primordial characteristics of the CLBL-1 cell line prove the integrity of a canine B-cell lymphoma in a murine in vivo model. *PLoS One.* 2012; 7(6):e40078. [PubMed: 22761949]
34. Weiskopf K, Anderson KL, Ito D, et al. Eradication of canine diffuse large B-cell lymphoma in a murine xenograft model with CD47 blockade and anti-CD20. *Cancer Immunol Res.* 2016;4(12): 1072–1087. [PubMed: 27856424]

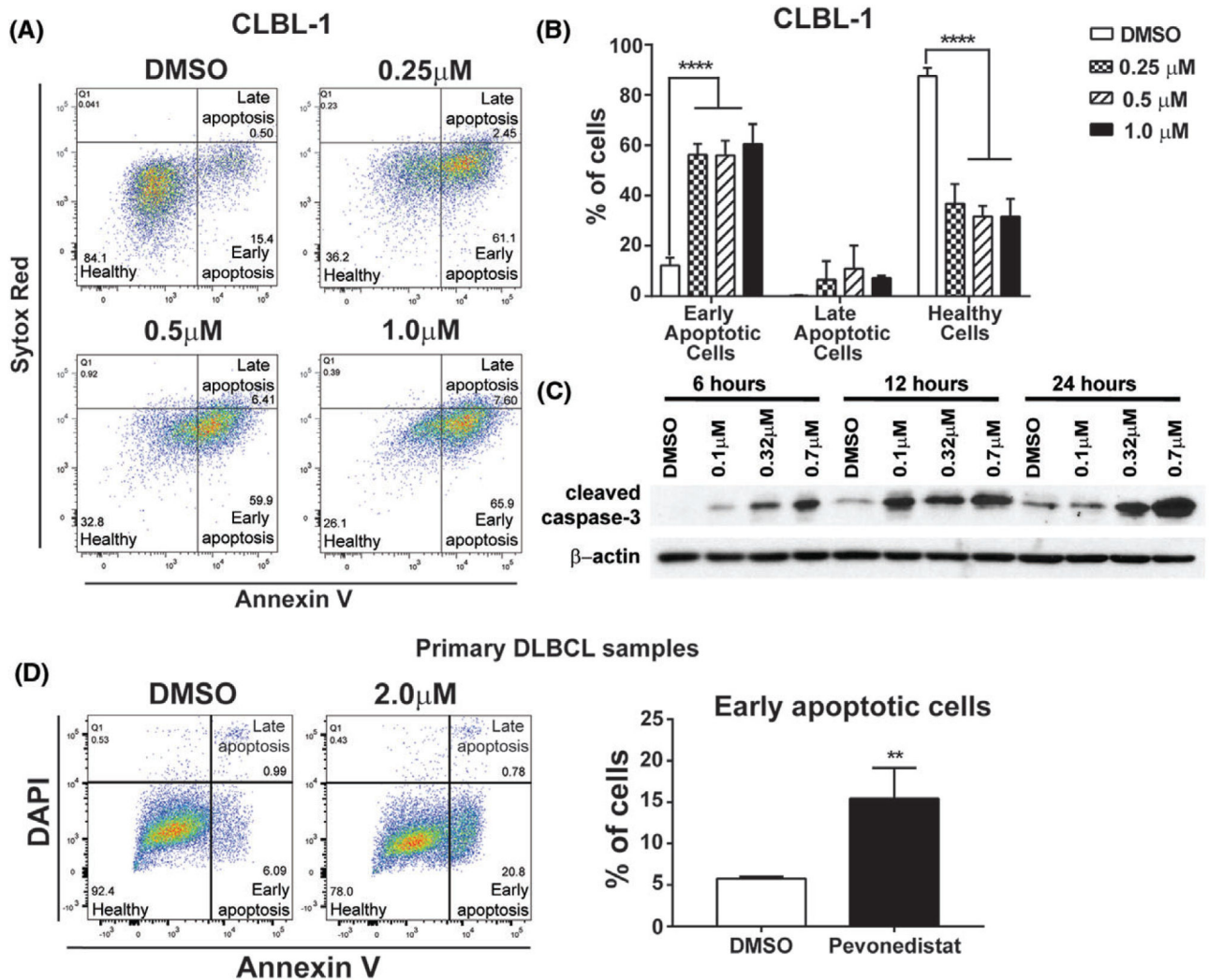
**FIGURE 1.**

Pevonedistat inhibits canine diffuse large B-cell lymphoma cell growth. A, Trypan blue exclusion assay. B, CellTiter96 AQueous one solution cell proliferation assays. C, IC<sub>50</sub> and IC<sub>90</sub> of pevonedistat in CLBL-1 cells after 72-hours pevonedistat treatment. DMSO-treated cells were used as an internal control. The percentage of growth was normalized to the DMSO-treated control group. \* $P < 0.05$ ; \*\*\* $P < 0.001$ ; \*\*\*\* $P < 0.0001$ . Data was presented as mean  $\pm$  SD

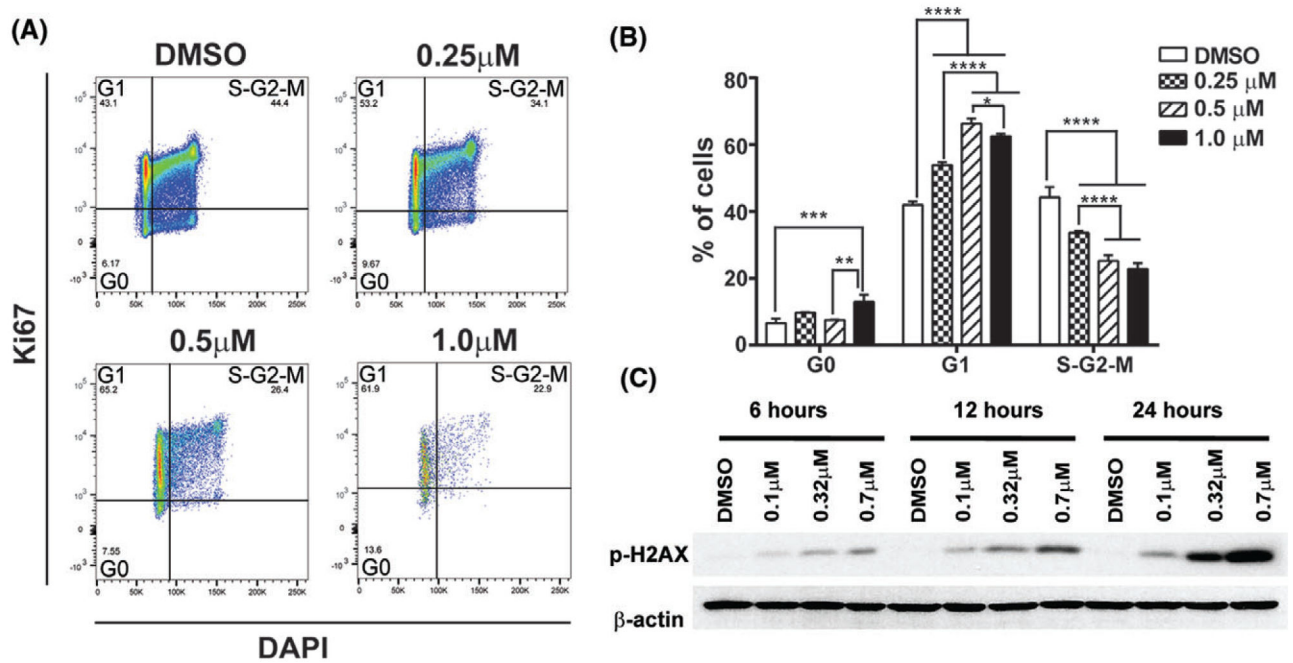
**FIGURE 2.**

Pevonedistat decreases cell viability of primary canine large B-cell lymphoma samples. A, CellTiter96 AQueous one solution cell proliferation assays show that pevonedistat decreases the viability of four primary canine lymphoma samples. B, MTS assay of three canine normal lymph node samples. The percentage of growth was normalized to the DMSO-treated control group. \*\*\*\* $P < 0.0001$ . Data was presented as mean  $\pm$  SD

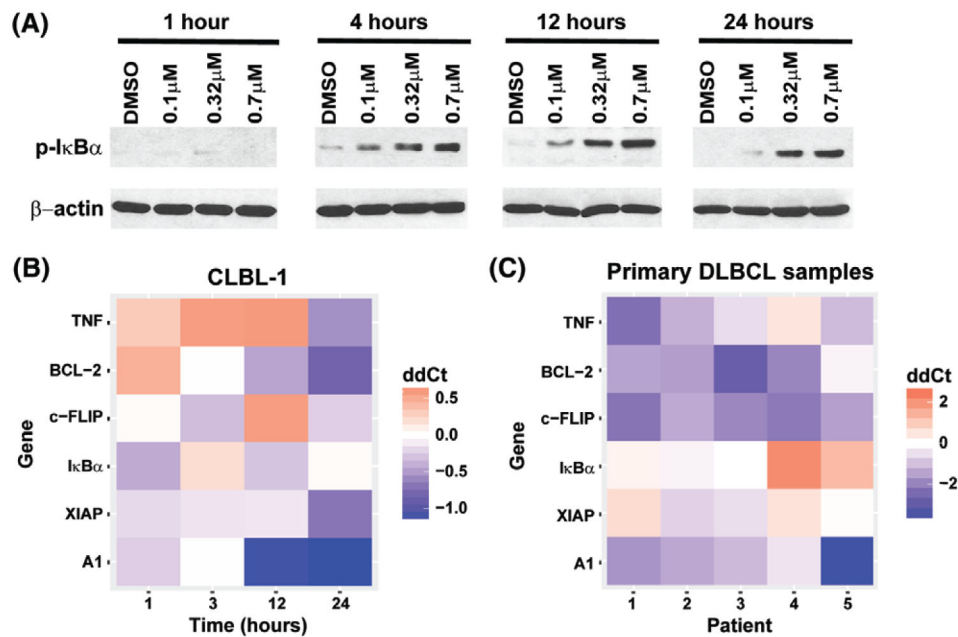


**FIGURE 3.**

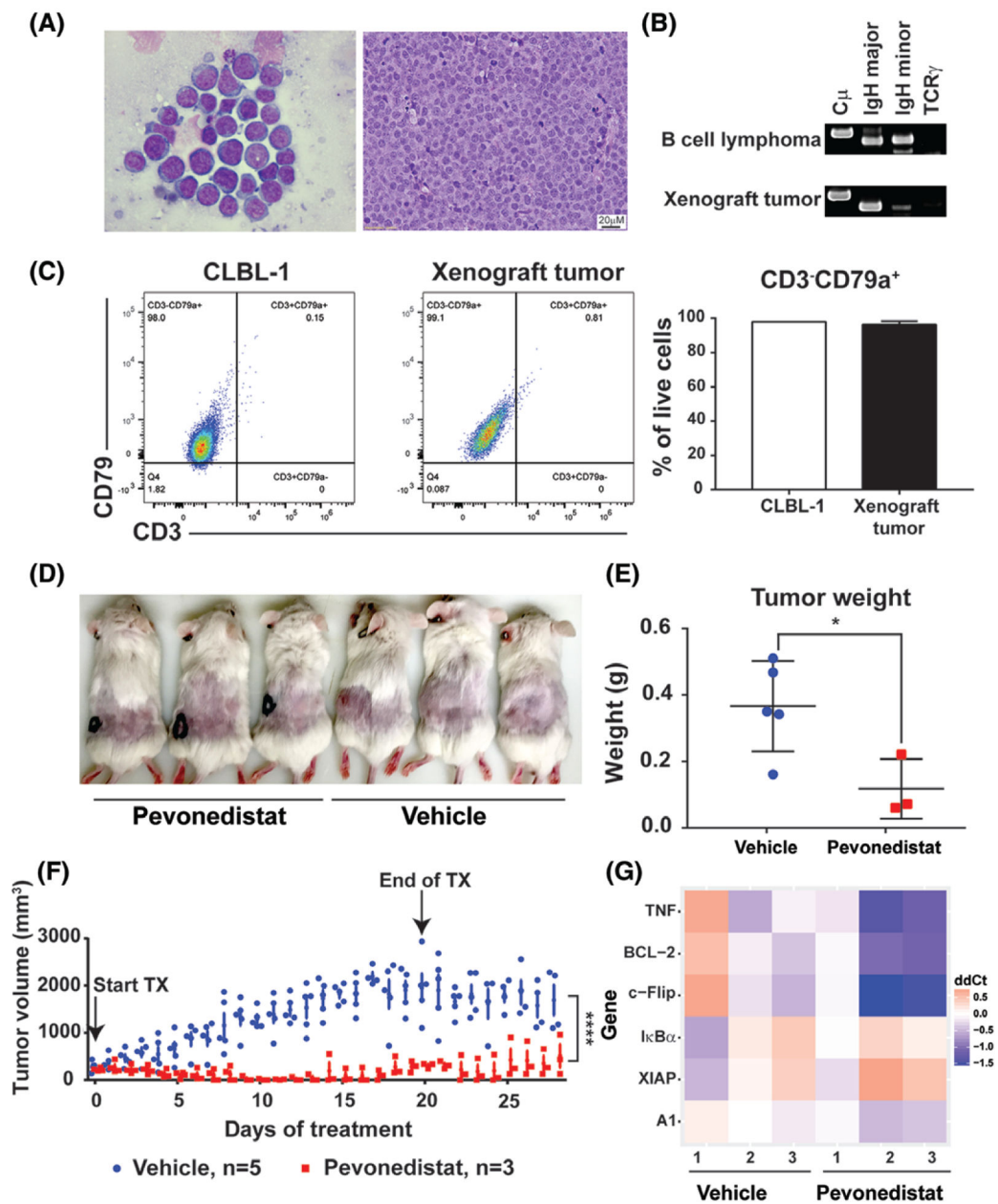
Pevedonidstat increases apoptosis in canine DLBCL. A, Representative gating strategy for flow cytometric analysis of pevedonidstat-treated cells for early apoptosis (Annexin V<sup>+</sup>, SYTOX red<sup>-</sup>), late apoptosis (annexin V<sup>+</sup>, SYTOX red<sup>+</sup>) and healthy cells (Annexin V<sup>-</sup>, SYTOX red<sup>-</sup>). B, Quantification of healthy, early apoptotic and late apoptotic CLBL-1. C, Western blot for cleaved caspase 3. CLBL-1 cells were treated with DMSO or pevedonidstat (0.1–0.7  $\mu\text{M}$ ) for 6, 12 and 24 hours. Cell lysates were immunoblotted for cleaved caspase3 expression.  $\beta$ -actin was used as a loading control. D, Representative gating strategy for flow cytometric analysis of pevedonidstat-treated primary canine DLBCL samples and quantification of early apoptotic cells. Early apoptotic cells were gated as Annexin V<sup>+</sup> DAPI<sup>-</sup>, late apoptotic cells were gated as Annexin V<sup>+</sup> DAPI<sup>+</sup>, and healthy cells were gated as Annexin V<sup>-</sup> DAPI<sup>-</sup>. \*\* $P < 0.01$ ; \*\*\*\* $P < 0.0001$ . Data was presented as mean  $\pm$  SD

**FIGURE 4.**

Pevonedistat treatment causes a G1-phase cell cycle arrest. **A**, Representative gating strategy for Ki67/DAPI cell proliferation assay. Cells in G0 phase were defined as Ki67<sup>-</sup>DAPI<sup>-</sup>. Cells in G1 phase were defined as Ki67<sup>+</sup> DAPI<sup>-</sup>. Cells in S/G2/M phase were defined as K67<sup>+</sup>DAPI<sup>+</sup>. **B**, Quantification of CLBL-1 cells in G0, G1 and S/G2/M phases 72 hours post-treatment. **C**, CLBL-1 cells were treated with DMSO or pevonedistat (0.1–0.7 μM) for 6, 12 and 24 hours. Cell lysates were immunoblotted for p-H2AX. β-actin was used as a loading control. \**P* < 0.05; \*\**P* < 0.01; \*\*\**P* < 0.001; \*\*\*\**P* < 0.0001. Data was presented as mean ± SD

**FIGURE 5.**

Pevedonidstat treatment inhibits NF- $\kappa$ B pathway. A, CLBL-1 cells were treated with DMSO or pevedonidstat (0.1–0.7  $\mu$ M) for 1, 4, 12, and 24 hours. Cell lysates were immunoblotted for p-I $\kappa$ B $\alpha$ .  $\beta$ -actin was used as a loading control. B, CLBL-1 cells were treated with IC<sub>90</sub> concentration (0.58  $\mu$ M) of pevedonidstat for 1, 3, 12 and 24 hours, NF- $\kappa$ B pathway target gene expressions were measured by qRT-PCR and were compared with the gene expression levels in cells treated with DMSO. Gene expression level in DMSO-treated cells were set as ddCt = 0. C, Canine primary DLBCL cells were treated with pevedonidstat for 24 hours, and NF- $\kappa$ B pathway target gene expressions were compared with DMSO control. Gene expression level in DMSO-treated cells were set as ddCt = 0. Each lane represents one patient sample

**FIGURE 6.**

Pevenedistat treatment leads to xenograft tumour regression. A-C, canine DLBCL murine xenograft tumour recapitulates canine large B-cell lymphoma in cell morphology, immunophenotype and cell surface expression markers. A, Cytologic and histologic analyses of xenograft tumour. B, PARR assay of xenograft tumour cells. Canine B-cell lymphoma sample was used as a positive control. C, Flow cytometry analysis and quantification of xenograft tumour cells and CLBL-1 cells. D, Representative image of xenograft mice with and without pevenedistat treatments. E, Tumour weight of vehicle and pevenedistat-treated mice. F, Tumour volume of vehicle and pevenedistat-treated mice. Arrows indicated the start of and the end of treatments. G, NF- $\kappa$ B pathway target gene expressions in xenograft tumours. After xenograft tumour formed, mice were treated with one dose of pevenedistat

(60 mg/kg) ( $n = 3$ ) or with one dose of vehicle ( $n = 3$ ). Xenograft tumours were harvested 48 hours post-treatment. \* $P < 0.05$ , \*\*\*\* $P < 0.0001$ . Data were presented as mean  $\pm$  SD

Author Manuscript

Author Manuscript

Author Manuscript

Author Manuscript